

Article

# Karst Development Mechanism and Characteristics Based on Comprehensive Exploration along Jinan Metro, China

Shangqu Sun <sup>1,2</sup>, Liping Li <sup>1,2,\*</sup>, Jing Wang <sup>1,2</sup>, Shaoshuai Shi <sup>1,2</sup> , Shuguang Song <sup>3</sup>,  
Zhongdong Fang <sup>1,2</sup>, Xingzhi Ba <sup>1,2</sup> and Hao Jin <sup>1,2</sup>

<sup>1</sup> Research Center of Geotechnical and Structural Engineering, Shandong University, Jinan 250061, China; sunshangqu@mail.sdu.edu.cn (S.Sun); wjingsdu@163.com (J.W.); shishaoshuai@sdu.edu.cn (S.Shi); 201613357@mail.sdu.edu.cn (Z.F.); 201714551@mail.sdu.edu.cn (X.B.); 201814644@mail.sdu.edu.cn (H.J.)

<sup>2</sup> School of Qilu Transportation, Shandong University, Jinan 250061, China

<sup>3</sup> School of Transportation Engineering, Shandong Jianzhu University, Jinan 250101, China; songsg@sdjzu.edu.cn

\* Correspondence: liliping@sdu.edu.cn

Received: 28 August 2018; Accepted: 19 September 2018; Published: 21 September 2018



**Abstract:** Jinan is the capital of Shandong Province and is famous for its spring water. Water conservation has become the consensus of Jinan citizens and the government and the community. The construction of metro engineering in Jinan has lagged behind other cities of the same scale for a long time. The key issue is the protection of spring water. When metro lines are constructed in Jinan karst area, the water-inrushing, quicksand, and piping hazards can easily occur, which can change the groundwater seepage environment and reduce spring discharge. Therefore, we try to reveal the development conditions, mechanism, and mode of karst area in Jinan. In addition, we propose the comprehensive optimizing method of “shallow-deep” and “region-target” suitable for exploration of karst areas along Jinan metro, and systematically study the development characteristics of the karst areas along Jinan metro, thus providing the basis for the shield tunnel to go through karst areas safely and protecting the springs in Jinan.

**Keywords:** Jinan metro; water conservation; karst exploration; development mechanism; shield tunnel

## 1. Introduction

With the rapid development of cities and urban population, traffic congestion has become one of the greatest problems in most cities in China. However, metro construction makes full use of underground space and reduces congestion on the ground. Therefore, metro construction has become the main form of urban infrastructure and traffic in China in the 21st century [1–7]. Until now, 53 cities have won the approval of rail transit planning, with a total length of about 8600 km. By the end of 2020, a total of 177 rail lines will be in construction, with a total operating distance of about 6100 km. Due to the complex urban geological conditions, a large number of metro tunnels run through karst geological areas. The existence of karst caves along the planning metro line can have great effect on the safety of tunnel design, construction, and operation [8]. Although several research on shield tunnelling in soft soils and sand and gravels have been conducted by many scholars [9–15], shield tunnel excavation in karst regions is rarely discussed.

Limestone geology is widely distributed throughout China. Moreover, seven primary karst areas can be concluded in China, each of which has its own characteristics. The common karst types include subterranean river-type caves, sink hole-type caves, through caves, phreatic caves along river valleys,

vadose caves, and tufa caves [16]. During the metro construction in karst areas, caves that have developed or are developing are often encountered, which pose great difficulties in tunneling by shield machine. As most of the karst caves are in non-filled, semi-filled, or rich muddy water-filled, a number of hazards including sink holes, karst collapse, and water inrush can easily occur in metro tunnel projects when they pass through karst areas [17,18].

Jinan City is located in Eastern China and is famous for its springs with complex groundwater network. Jinan overlooks the Mount Tai to the south and across the Yellow River to the north, as indicated in Figure 1. The structural unit of the northern foothills of Mount Tai, gradient from south to north, is accelerative for formation of spring water. After the atmospheric rainfall infiltrates into the soluble carbonate rocks, the water flows from south to north along the topographic trend, gathers in the connecting area of the monoclinic structure and the northern plain, and then crops out of the surface, forming a rising spring. The comprehensive conditions of strata, geological structure and hydrogeology lead to concealed karst caves, which can cause ground surface settlement and karst collapse, water inrush, mud inrush, and other hazards. The metro lines under construction in Jinan will inevitably go through karst areas, which contain rich groundwater and a large number of concealed karst caves. Karst caves will threaten the safe construction and stability of shield tunnel, especially when considering the complexity of groundwater in Jinan spring areas and the appeal for “protecting the spring”. Therefore, safe construction is particularly important in karst areas where Jinan Metro runs through.

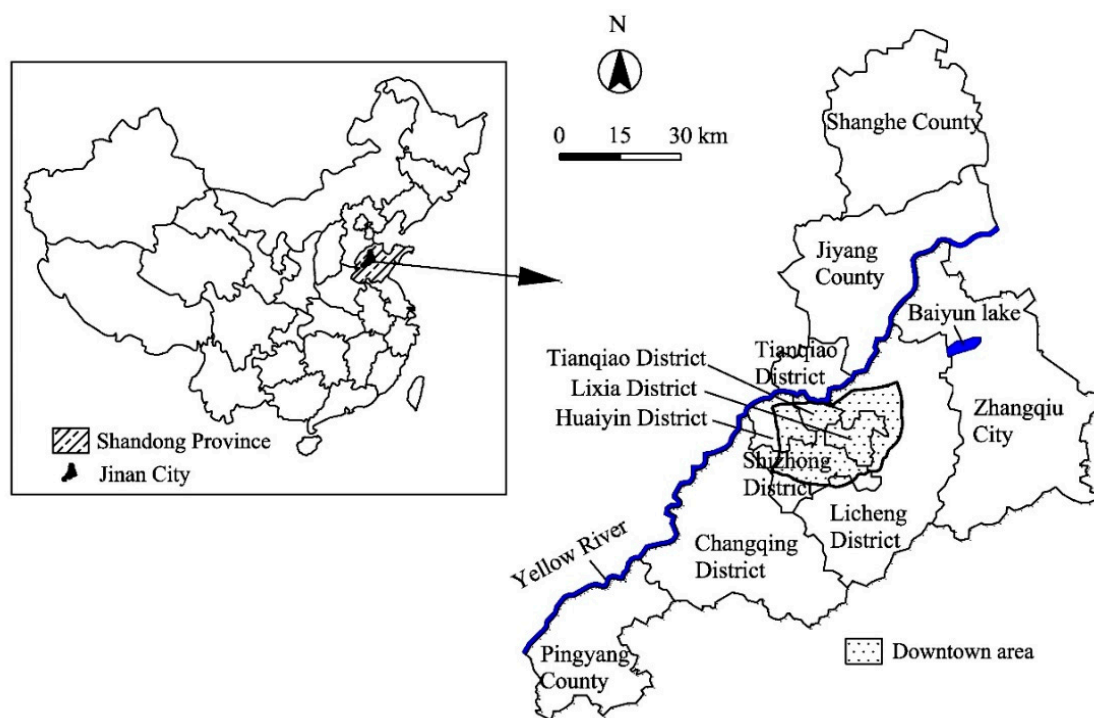


Figure 1. Overview of Jinan city [19].

This paper mainly focuses on the karst areas where R1 and R2 lines of Jinan Metro go through. The planning map of main metro lines is shown in Figure 2. After revealing the conditions and development mechanism of karst area in Jinan, we propose the comprehensive detection method of “shallow-deep” and “region-target” suitable for exploration of karst areas, and systematically studies the development scale and characteristics of karst areas along Jinan metro, thus providing the basis for the shield tunnel to go through karst areas safely.

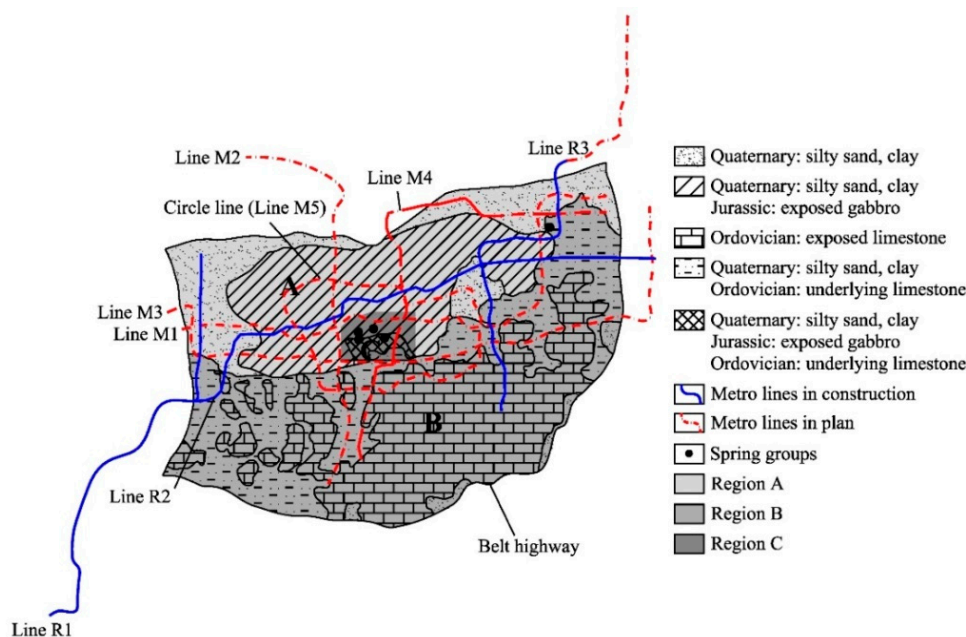


Figure 2. Jinan metro plan map [19].

## 2. Karst Development Conditions and Mechanism along the Jinan Metro

The karst development is mainly controlled by the solubility of rocks, geological structures (including rock strata, faults, fissures, etc.), and groundwater [20–25]. Among them, the fluidity of water is the most active factor. According to the special hydrogeological conditions in Jinan, the factors affecting karst development can be divided into four categories: topography, formation lithology, groundwater action, and geological structure.

### 2.1. Topography

The terrain of Jinan is high in the south and low in the north, with small mountain ranges in the east and west sides, forming a unique semi-basin landform. The southern part of Jinan is a hilly area, while the northern part is near the Yellow River. The urban area in Jinan is located in the piedmont plain. The highest elevation of the southern mountains is approximately 1108.4 m, while the lowest elevation in the north is about 5 m, leading to the elevation difference of about 1100 m. Owing to gravity, the groundwater flows from south to north. In addition, several mountains are located along the east-west direction, blocking the flow and diffusion of groundwater. As a result, the groundwater runs from three directions, accelerating its flow and exacerbating the karstification.

According to the geomorphological characteristics of Jinan, the city is divided into classification I containing plain and mountain, and classification II, which contains five more specific categories, as shown in Table 1. The terrain turns from high to low from south to north. The types of landform genesis are low mountain area, monadnock-hilly area, alluvial-diluvial plain area, alluvial plain area, and dissolved monadnock area, as shown in Figure 3.

Table 1. Terrain classification.

Classification I		Classification II
Plain	Accumulation	Alluvial Plain Alluvial-Diluvial Plain
	Mountain	Erosion
Karst		Dissolved Monadnock

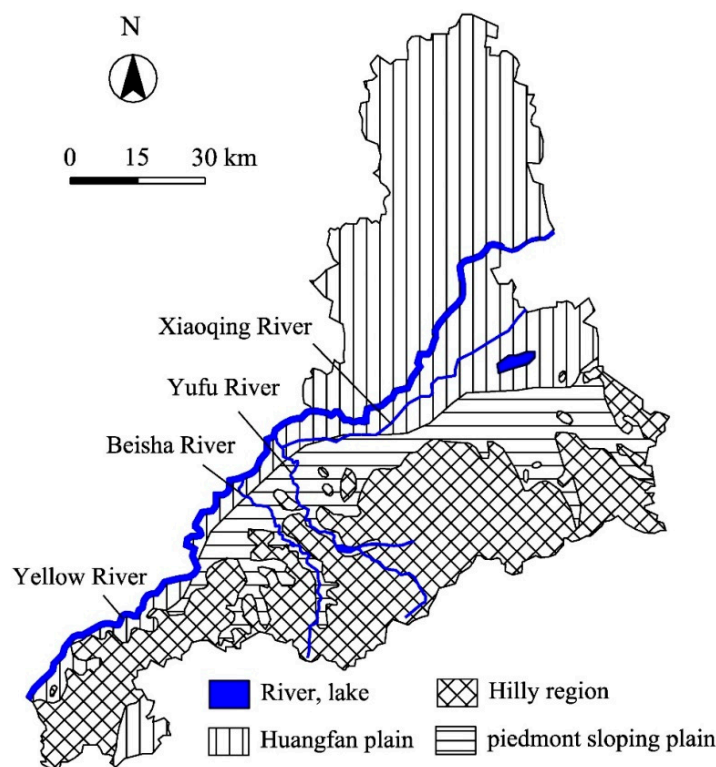


Figure 3. Geomorphologic map of Jinan city [19].

### 2.2. Formation Lithology

It can be seen from Figure 3 that the mountainous region is located mainly in the south and the plain region is situated mainly in the north of Jinan City. Based on the lithology, the hilly area can be divided into three subareas, including metamorphic rocks, carbonatite rocks, and magmatite rock. The first subarea distributes in the southwest of Zhangqiu city, southeast of Changqing County. The second subarea is located mainly around the first subarea. The third subarea is situated in the northeast of Zhangqiu city. In the second subarea, the minerals of carbonate rocks in the study area are mainly calcite and dolomite, and the chemical components are mainly CaO and MgO, which are soluble. The mineral and chemical compositions are the basic conditions to determine to what extent the karst develops. In accord with the topography, the plain region can be divided into two categories: the Huangfan Plain and the piedmont sloping plain. Huangfan Plain is situated mainly along Yellow River and the thickness becomes deeper from south to north. The main stratigraphy consists of silty sand, clay, sandy loam, and mucky soil. The piedmont sloping plain is located in the center of Jinan, which belongs to the piedmont alluvial plain. The stratigraphy includes clay, sandy loam, and gravel with mud. Several small buttes can be found on the piedmont sloping plain, caused by the intrusion of gabbro in the Yanshan period.

### 2.3. Hydrogeological Environment

The hydrogeological map of Jinan City is shown in Figure 4. Four aquifer groups can be found in the study area, including a Quaternary porous aquifer group (AqP), a karst aquifer group (AqK), an interbedded karst-fissure aquifer group (AqKF), and a fissure aquifer group (AqF). The four aquifer groups are connected to each other in the whole groundwater circulation. In the karst aquifer group, a wide range of carbonate rocks are deposited, including limestone and dolomite formed in the Cambrian and the Ordovician period. Therefore, the karst area is well-developed. Soluble carbonatites can be dissolved and corroded, which will result in a large number of pores, fissures, grikes, and karst caves.

The soluble rock can be dissolved by the solution of water. Water's ability to dissolve is derived from bicarbonate ( $\text{HCO}_3^-$ ), which is formed through combination of carbon dioxide ( $\text{CO}_2$ ) and water, and can dissolve carbonate rocks under long-term reactions. In addition, due to the flow of groundwater, transportation will expand the scale of karst development. Among the chemical components of karst water near the exposed spring water, the cation is mainly  $\text{Ca}^{2+}$ , with content of 80–123 mg/L, followed by  $\text{Mg}^{2+}$ , with content of 15–24 mg/L; the anion is mainly  $\text{HCO}_3^-$ , which is 171–338 mg/L, followed by  $\text{SO}_4^{2-}$ , with content of 3–107 mg/L. The mineralization is 492–699 mg/L; the total hardness is 262–405 mg/L; the PH value is between 7.1–7.8;  $\text{HCO}_3^-$  water is the only chemical type of the karst water, which has good quality, therefore, can present overall characteristics of the karst water.

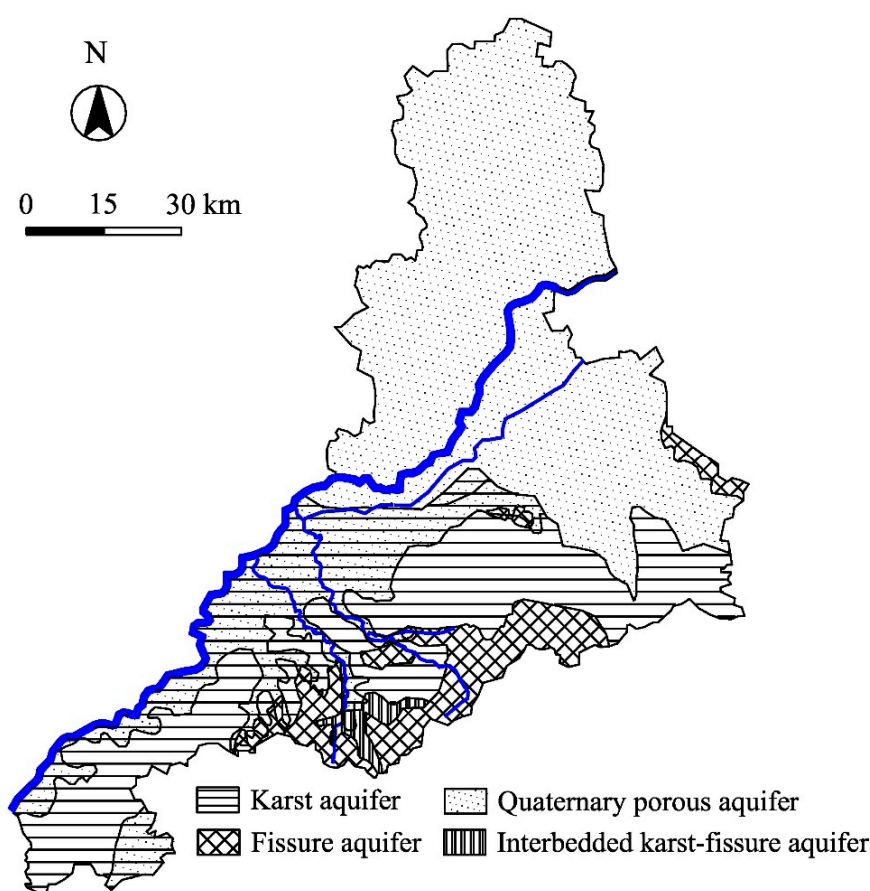


Figure 4. Hydrogeological map of Jinan [19].

#### 2.4. Structural Influence

Jinan area is generally a north-dipping monoclinic structure dominated by Paleozoic strata, with a number of east-west small folds and faults. There are also many structural joints and cracks influenced by quartz veins. The erosion of water on rockmass generally begins with joint fissures, and the karst is developing with the crack expansion. Therefore, the development degree and extension direction of fissures usually control the extent and direction of karst development.

In the northern part of the monoclinic structure, there are extensive magmatic activities. In the southern part of the monoclinic structure, the crystalline basement of the Archean gneiss is widely exposed, with Paleozoic strata. There are developed regional faults but few folds and magma activities. The dip angle is gentle. In the monoclinic structure, a number of large-scale North and Northwest trending faults grow, together with Northeast trending faults. The North and Northwest trending faults are distributed roughly equidistantly from east to west, dividing the monoclinic structure into several fault blocks, which play important roles in the hydrogeological conditions in the area.

As shown in Figure 5, the four typical faults are F1 (Mashan Fault), F2 (Qianshan Fault), F3 (Dongwu Fault), and F4 (Wenzuxin Fault).

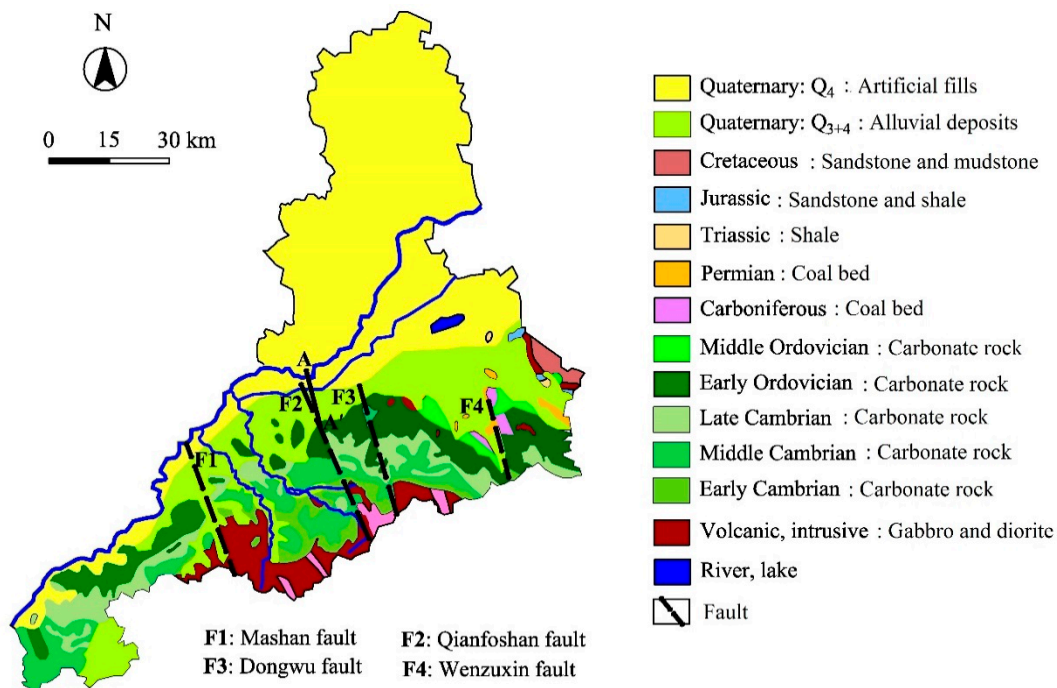


Figure 5. Jinan city geological map (modified after [19]).

### 2.5. Karst Development Mechanism along the Metro Lines

Instead of a single reaction, the multiple factors influencing karst development affect each other and result in various feedbacks. The interaction mechanism and mutual feedback system of the multiple factors have been summarized according to the karst conditions of Jinan Metro, as shown in Figure 6. The karst water in Jinan mainly comes from atmospheric precipitation. The climatic factors including temperature, amount of rainfall and evaporation all affect the precipitation. They replenish the groundwater system directly. Additionally, the chemical action of soluble rock is generated by precipitation. The terrain of Jinan, which is higher in the south and lower in the north, promotes the overall flow of karst water. The geological structures, including the fault zone, fault, fracture zone and the development degree and orientation of the rockmass fissure, determine to what extent the karst develops. The combined action of the factors mentioned above determine the flow velocity and hydraulic characteristics of karst water in Jinan area, the result of which affects karstification in turn, thus forming the overall interaction relationship and development mechanism of karst in Jinan area.

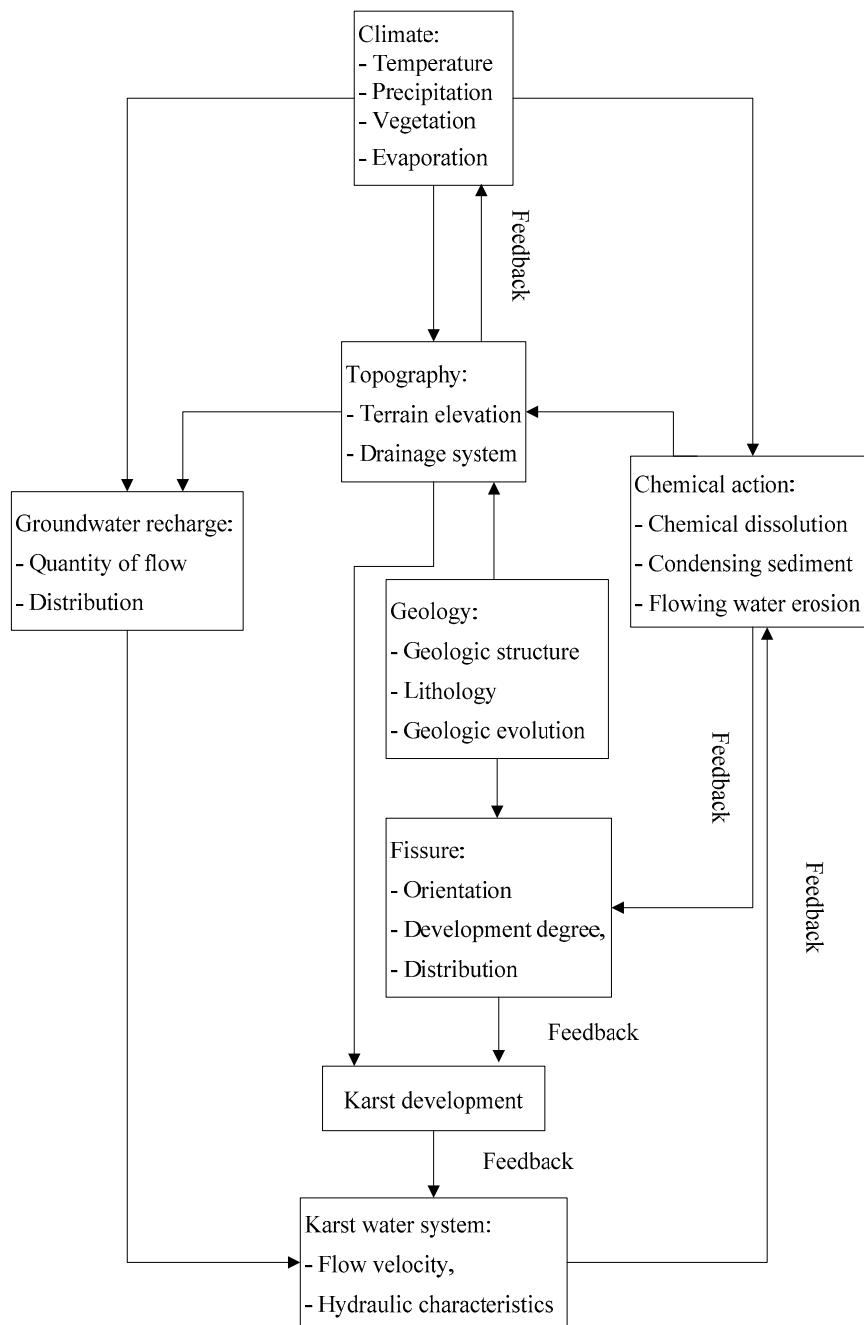


Figure 6. Karst development mechanism along the metro lines.

### 3. Karst Development Mode along the Metro

Karst is a general term for grooves, fissures, and caves caused by the chemical and physical effects of water on soluble rock formations, including carbonate strata (limestones and dolomites), sulfate strata (gypsum), and halogen strata (rock salt), and phenomena produced by these effects. The nature of karst is chemical action, that is, chemical erosion of water on rock. Karst development is the evolution under the comprehensive conditions of geological structure, groundwater action, soluble rock, and topography.

Jinan area is dominated by karst water. The karst groundwater mainly comes from the southern mountainous area, where the karst landforms develop, thus forming karst erosion. Typical karst forms include karst caves, karst depressions, groundwater channeling, and solution cracks. The southern mountainous area is exposed limestone with some parts having thin overlying soil. Moreover,

developed karst fissures are widely distributed. Thus, karst water channels and water storage spaces are easily formed. In addition, the special terrain of Jinan can promote the flow of karst water from south to north along the strata and tectonic belts. The urban area is mainly composed of the inclined piedmont plain and a small part of exposed limestone area. Compared with the southern hilly area, the overlying Quaternary strata are thicker and the depth of some local area can reach 100 m. The atmospheric precipitation enters the underlying limestone stratum through pore water, leading to karst dissolution and erosion, which produce karst water. At the bottom of the Quaternary strata, there are obvious red loess and mucky clay water-resisting layer, which has the characteristics of confined water. Therefore, the karst development models in Jinan can be divided into direct karst, indirect karst and confined karst.

Direct karst refers to the phenomenon that atmospheric precipitation directly supplies the exposed limestone area, where a shallow karst zone is formed due to fracture development and crush caused by long-term weathering and dissolution, and that the karst infiltrates through limestone fissures, leading to karst channel, as shown in Figure 7a. In the limestone strata, the closed fissures have poor permeability, while the open cracks have high permeability. The open cracks are directly exposed to air and precipitation, intensifying the chemical dissolution, thus resulting in karst depressions, which, to some extent, changes the direction of karstification. In addition, owing to the special terrain of Jinan area, the karstification presents a vertical direction and a horizontal direction from south to north, as shown in Figure 7b. The direct karstification is mainly located in the southern hilly areas in Jinan. The generalized model is shown in Figure 7c. The karst water here has the characteristics of a phreatic layer.

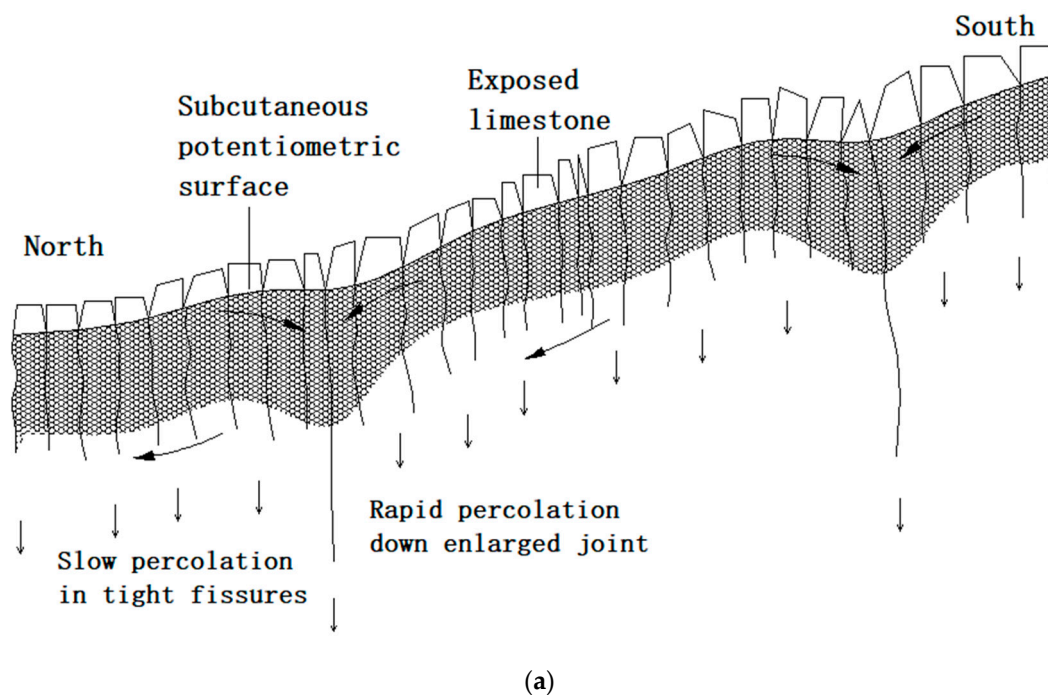
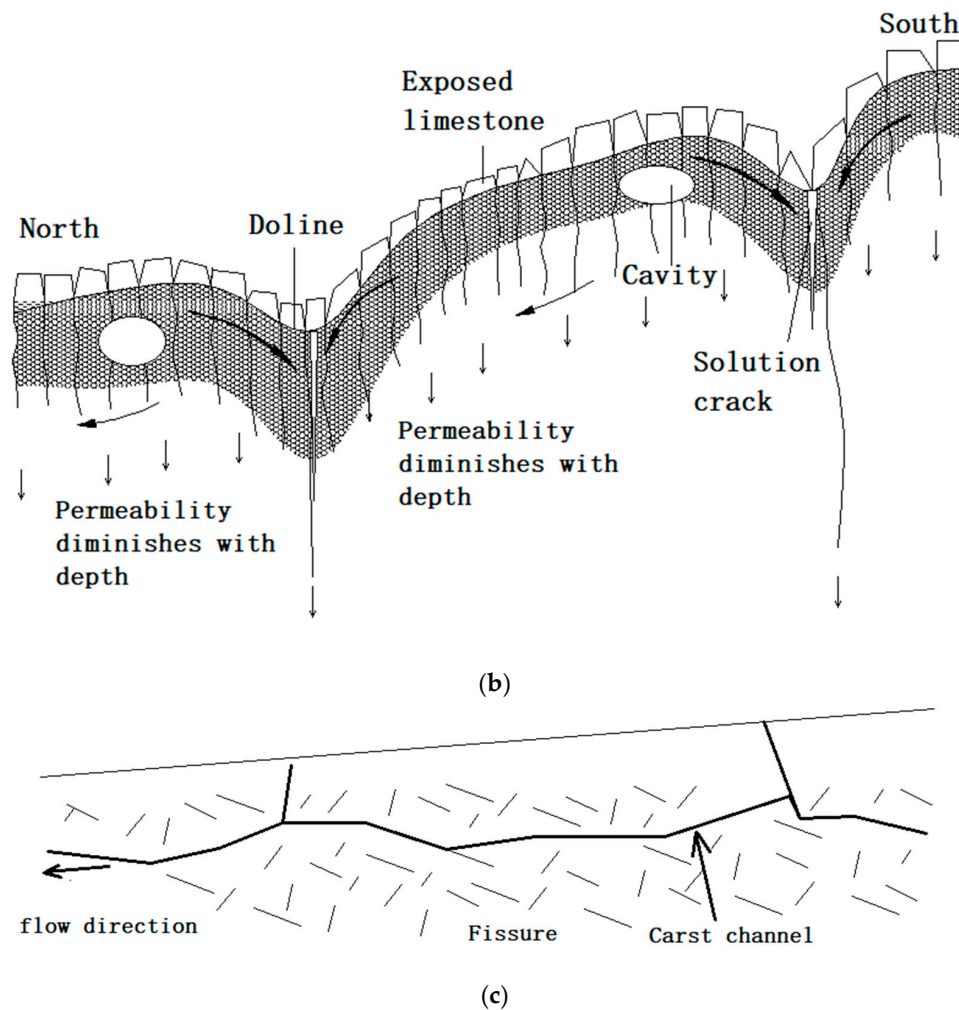


Figure 7. Cont.



**Figure 7.** The evolution of direct karst development in Jinan: (a) Primary stage; (b) Evolution process; (c) Simplified model.

The indirect karst strata mainly include (I) overlying Quaternary strata and (II) soluble limestone strata, and its development evolution is shown in Figure 8. As revealed in Figure 8a, the atmospheric precipitation directly replenishes the overlying Quaternary strata and is collected as pore water into the underlying limestone strata. According to the fissure development and the permeability, limestone strata can be divided into closed fracture low-permeation zone and open fracture quick-permeation zone. Water is extremely easy to be stored in the open fracture. Therefore, the karst dissolution and erosion are more intense, accelerating karst water seepage, resulting in karst depression, see Figure 8b. The fracture opening of limestone strata and the permeability decreases with the increase of depth, except for the widened infiltrating main fracture and fault. As a result, surface precipitation is easy to store in shallow limestone fissure zone, especially during the rainy season. The special terrain of Jinan and karst depressions often change vertical karstification into horizontal. The overall direction of karstification, however, remains vertical and horizontal from south to north. Karstification also leads to typical formations including karst caves, dissolution cracks, and groundwater channeling. The generalized model of indirect karst development is shown in Figure 8c. The limestone strata receive precipitation from the overlying Quaternary strata, and the infiltrating main channel is formed in the fracture concentrating zone with larger opening or fault structure. Then, the water head difference caused by the topography enhances horizontal development of karst, forming karst channels in the fracture development zone, which has the characteristics of a phreatic layer. Indirect karst is mainly located in the inclined piedmont plain.

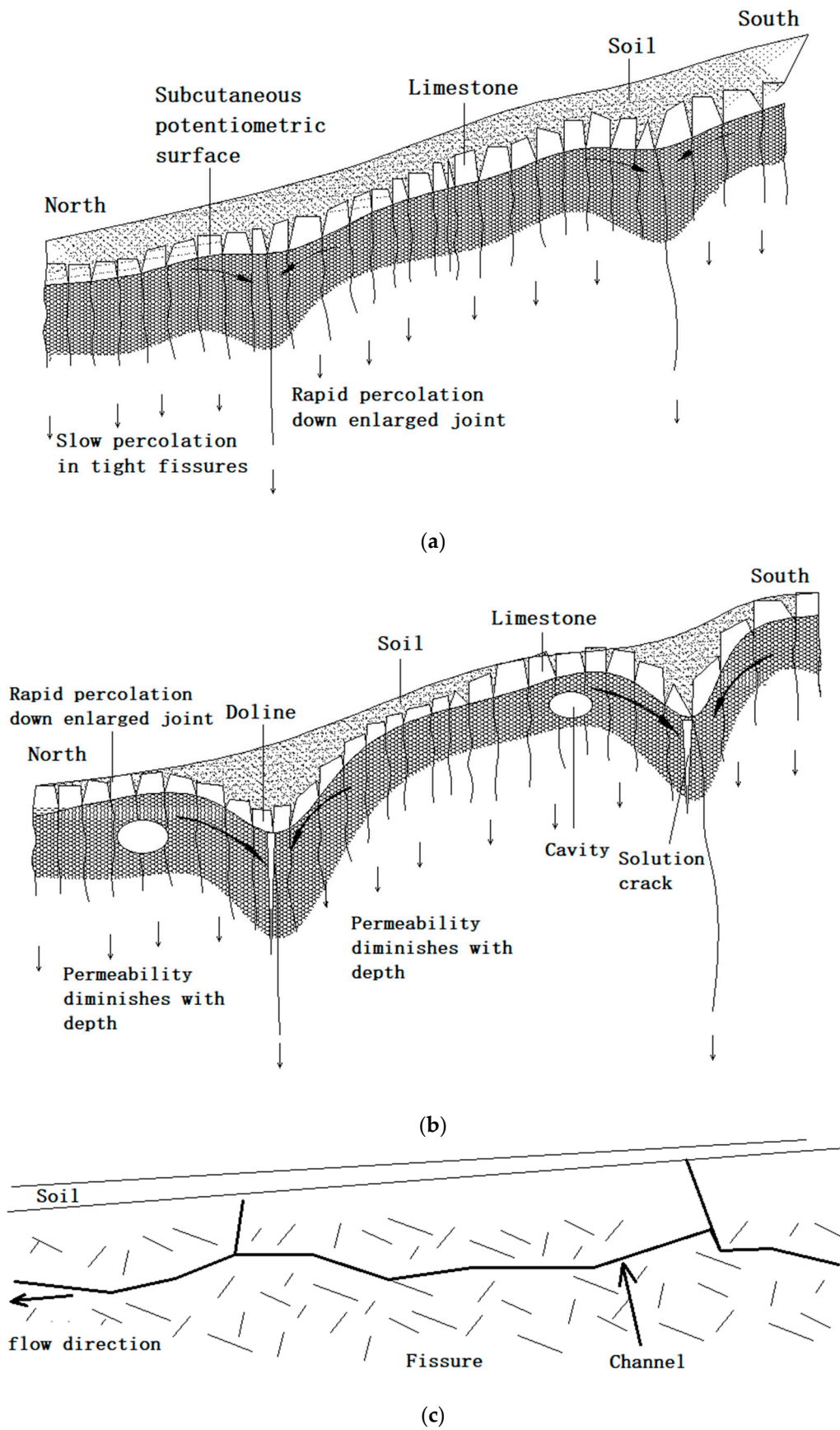
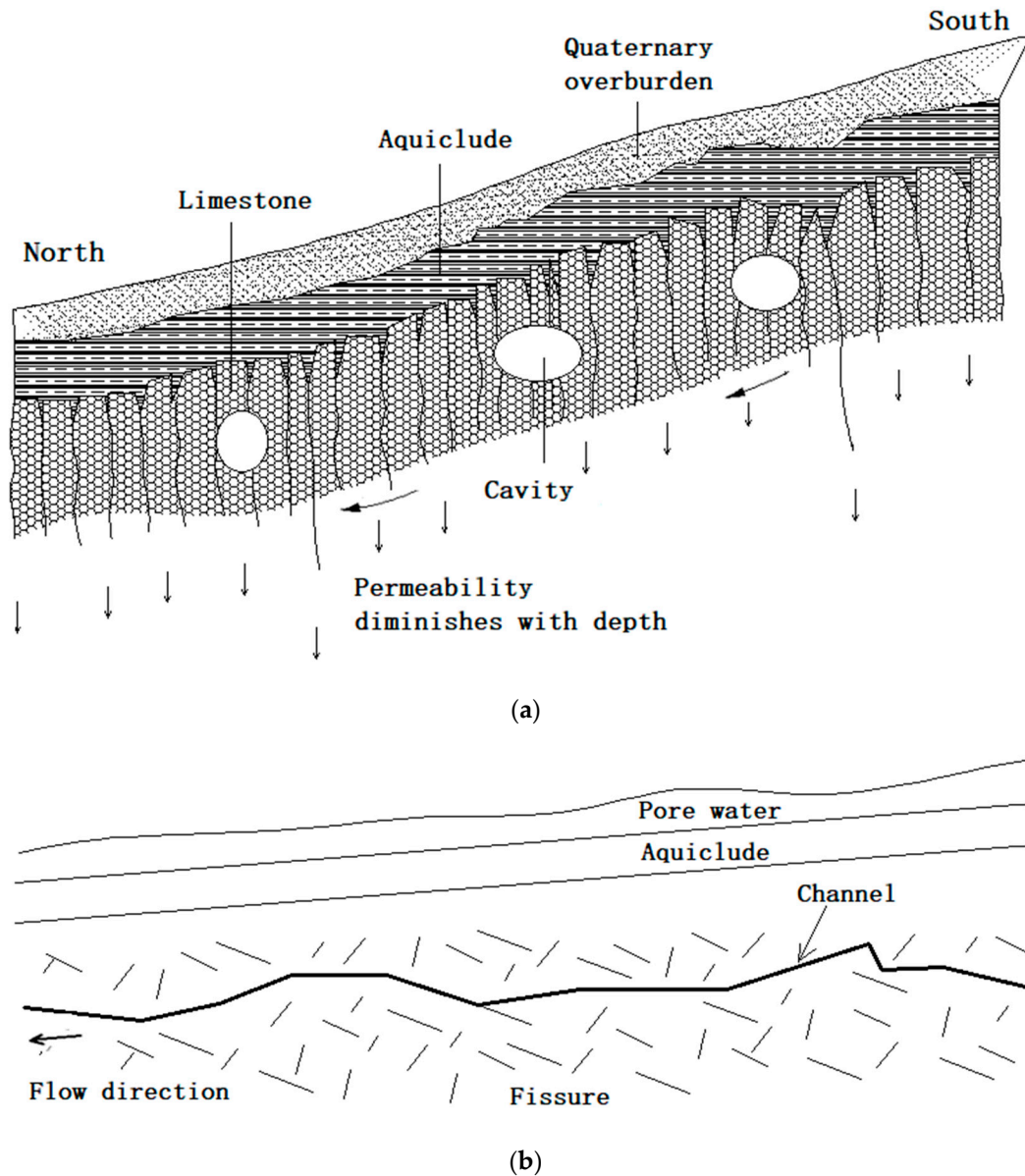


Figure 8. The evolution of indirect karst development in Jinan: (a) Primary stage; (b) Evolution process; (c) Simplified model.

As for the confined karst, there are water resisting layers with red loess and mucky clay in the overlying Quaternary strata and limestone strata, cutting hydraulic connection between the overlying pore water and the underlying karst water, as shown in Figure 9a. Consequently, the karst water has the property of confined water. Only in some locations, water-proof aquifer misses, forming skylight, where the pore water is in close hydraulic relationship with the karst water. The confined karst is mainly distributed in alluvial-diluvial plain areas of Jinan. Such karst water is blocked by igneous rocks in the north, forming horst structure, leading to spring water groups. The generalized model is shown in Figure 9b.



**Figure 9.** The evolution of confined karst development in Jinan: (a) Evolution process; (b) Simplified model.

#### 4. Karst Development Characteristics along Jinan Metro

At present, R1 line of Jinan metro has been successfully completed, and R2 line are under construction. Characteristics of the karst development areas of the above lines have been counted, summarized, and analyzed in this paper, in order to establish mechanisms of forming the karst area where Jinan metro runs through.

#### 4.1. Number of Karst Caves at Various Heights

As for R1 line, there are 71 drill holes exposed by karst caves among 145 exploratory holes, the proportion of which is 47.7%, and the total number of karst caves exposed is 129. Among them, 79 karst caves are smaller than 1 m and 50 larger than 1 m; 29 karst caves are larger than 2 m, 23 karst caves larger than 3 m; 12 karst caves are larger than 5 m. During the section between Renjiazhuang Station and Lashan Station in R2 line of Jinan metro, there are 97 drill holes exposed with limestone, and 26 drill holes exposed with karst caves, with the proportion of 26.8%. The overall height of karst caves are shown in Table 2.

**Table 2.** Number of karst caves at various heights.

Range of Height(m)	Numbers of Karst Caves	Proportion (%)
0–1	114	60.32
1–2	34	17.99
2–3	10	5.29
3–5	16	8.47
5–7	8	4.23
7–9	3	1.59
9–11	2	1.06
11–13	1	0.53
13–15	1	0.53
In Total	189	100.00

The diagram of the karst cave height was drawn, as shown in Figure 10. It can be seen that the caves in the karst area along the Jinan metro are mainly small- and medium-sized ones, and that karst caves with height less than 2 m account for 78.31%, and with height between 3 m to 5 m account for about 10%. In addition, a small number of large-sized caves are developed, and the maximum height of exposed karst cave is 13.2 m.

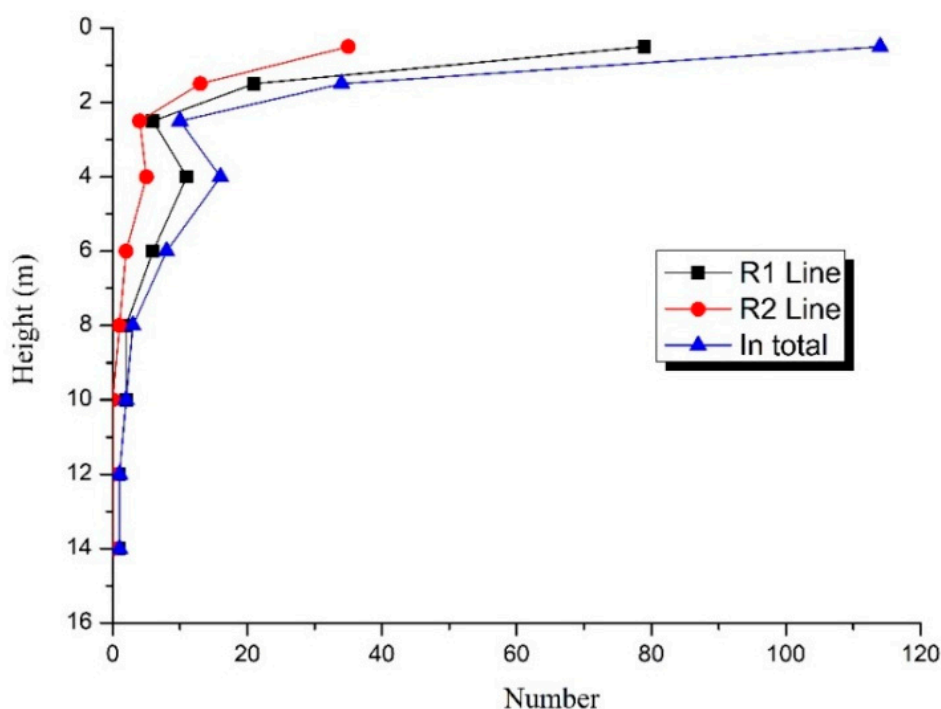


**Figure 10.** Number of karst caves at various heights.

#### 4.2. Filling Types of Karst Cave

Taking the exposed karst caves of R1 line as an example, there are 129 karst caves exposed by drill holes. Among them, there are 117 filled and semi-filled caves, accounting for 90.7%, and 12 caves without fillings, accounting for about 9.3%. Thus, the majority of karst caves are filled and semi-filled ones. The fillings are mainly cohesive soil, earth and rubble. Among them, 44 caves are filled with cohesive soil, accounting for 34.11%; 60 caves with earth soil, accounting for 46.51%; 13 caves with rubble, accounting for 10.08%; 12 caves with water or nothing, accounting for 9.3%. Karst caves with typical fillings and without fillings can be seen in Figure 11. The non-filled and water-filled karst caves are mostly developed in deep limestone strata. The water-filled karst caves are full of confined water. The flow of groundwater accelerates the erosion of karst fissure water, greatly affecting the stability of shield tunnels.

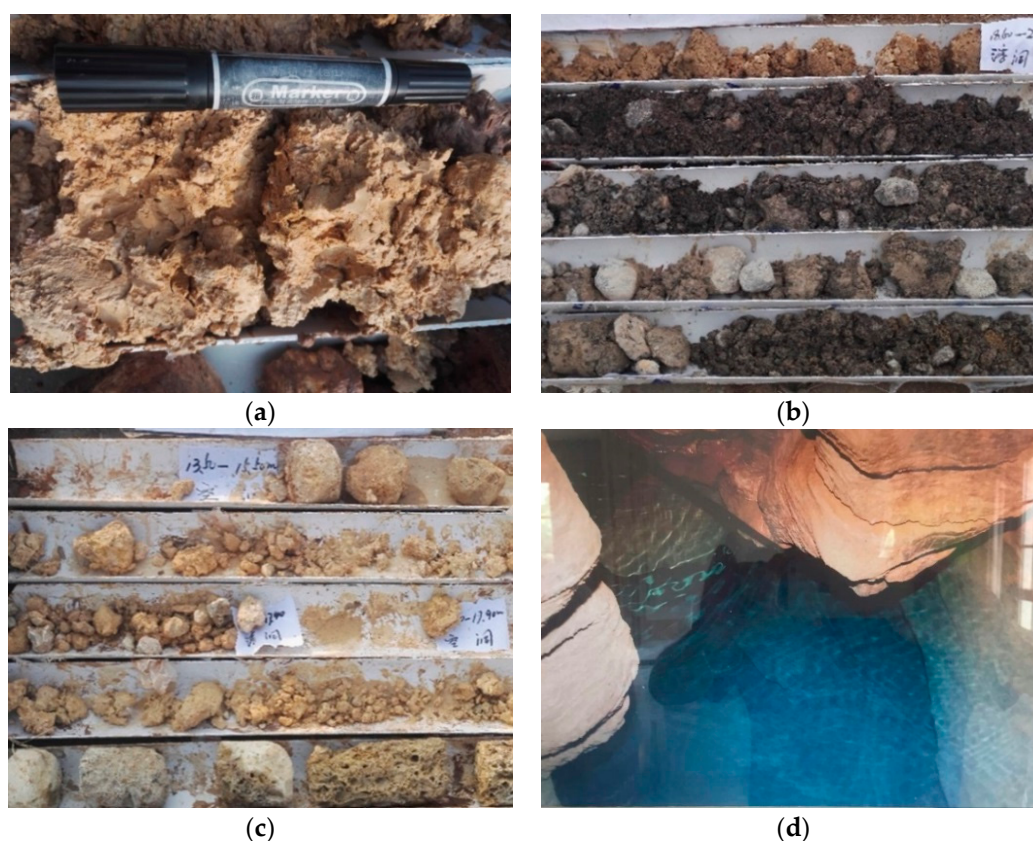


**Figure 11.** Typical fillings of karst caves: (a) Cohesive soil filling; (b) Earth filling; (c) No filling; (d) Water filling.

### 5. Study on Spatial Distribution Characteristics of Karst Based on Borehole and Integrated Geophysical Exploration

#### 5.1. Exploration of Abnormal Karst along Jinan Metro

In terms of conventional shallow karst area explorations, drilling exploration has obvious advantages for lithological discrimination, stratum structure, and key area checking. The geophysical exploration has large-scale detecting area and relatively high precision owing to various methods complementing each other. Most karst areas along the Jinan metro are covered with Quaternary strata, with limestone developed strata and abundant groundwater below. In light of this, comprehensive selection of “shallow-deep” and “region-target”, which is suitable for exploration of karst areas along Jinan metro, has been proposed. Firstly, Ground Penetrating Radar (GPR) method, which has high precision and fast efficiency for close exploration, was adopted to detect the soil hole

and stratum distribution in the shallow overlying Quaternary strata. Secondly, considering the intense karstification of limestone and rich water along the Jinan metro lines, the high density resistivity method and transient electromagnetic method were used due to the differences in electrical conductivity and resistivity between surrounding rocks and karst caves. The high density resistivity method is obviously effective on unfilled or water-filled karst caves which have significant electrical difference with surrounding rock. The rock resistivity is determined by, apart from the mineral composition of the rock, factors including water content and temperature. When there are cracks or fault zones in the underground rock and water-rich strata with water-conducting channels, the resistivity of rocks in these areas will be significantly reduced, and obvious electrical differences with the surrounding strata will be presented. Since each geophysical method has its own advantages and corresponding disadvantages, it is often difficult to meet the requirements of accuracy by applying a single method. Nevertheless, a combination of multiple geophysical methods can complement each other. The transient electromagnetic method has obvious advantages in finding low-resistance targets among high-resistance geological bodies. The electrical and electromagnetic methods were incorporated to define abnormal karst areas. Finally, in the crucial karst areas identified by the above methods, the cross-hole resistivity CT method and laser scanning were adopted for detailed detection. The comprehensive detecting method of “shallow-deep” and “region-target” is shown in Figure 12.

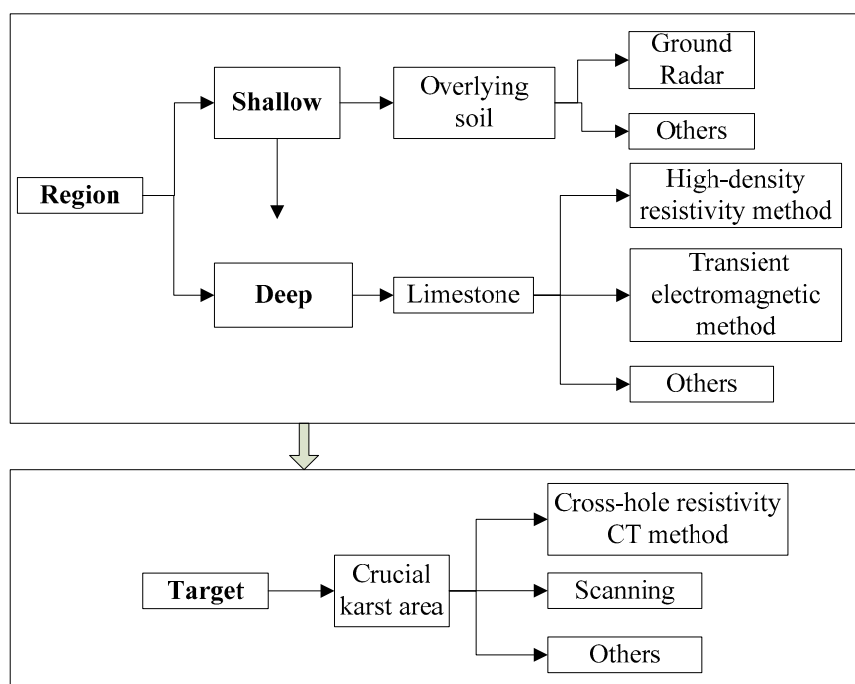


**Figure 12.** Comprehensive exploration system along Jinan metro.

Taking the section between Wangfuzhuang Station and Dayangzhuang Station along Jinan metro R1 line as an example, general detection by methods of GPR, high-density resistivity and transient electromagnetic was first conducted. Then, after initial interpretation of detecting results, detailed exploration was carried out for some key areas with cross-hole resistivity CT method and laser scanning. The corresponding geophysical results can be seen in Figure 13a–e, respectively. Figure 13a shows the potential cave through the GPR, but the detection depth can only reach about 10 m due to the absorption effect in overlying soil. According to the interpretation result of transient electromagnetic apparent resistivity, the karst in the area is strongly developed, with depth basically below 15 m, highly coincident with buried depth of the tunnel. The main areas of karst development and zone are circled by red dashed line in Figure 13b. Additionally, it is inferred through the distribution features

of apparent resistivity of five measuring lines that there are east-west karst and fracture zone in the middle of the detection area, as shown from AB-CD range in Figure 13c.

In order to further determine the development size of the karst cave in the potential karst development zone, the detailed detection by cross-hole resistivity CT method was carried out, and five abnormal karst caves were found. Combined with the corresponding geological and drill hole analysis, it is deduced that the abnormalities of R1-1, R1-2, R1-3, and R2-1 are water-rich caves or fractured areas, and that R2-2 is a semi-filled cave, as shown in Figure 13d. The previous geophysical survey conducted 2d detection from the whole and local areas. In order to obtain the three-dimensional spatial distribution of the karst caves and provide more accurate guidance to the construction department, CALS (Cavity Auto Scanning Laser System) made by MDL company was adopted to carry out 3d laser scanning of the caves through two boreholes, and the location of the borehole was marked in Figure 12d. The specific karst cave morphology are shown in Figure 13e. Compared with transient electromagnetic detecting results, the cross-hole resistivity CT and scanning method achieves detailed detection of water-rich caves. In terms of overall distribution of resistivity, compared with the CT results, the left low-resistance area is larger than the right, and the buried depth of karst development is shallow on the left and deep on the right. The results shows that multiple detection methods are in good agreement.

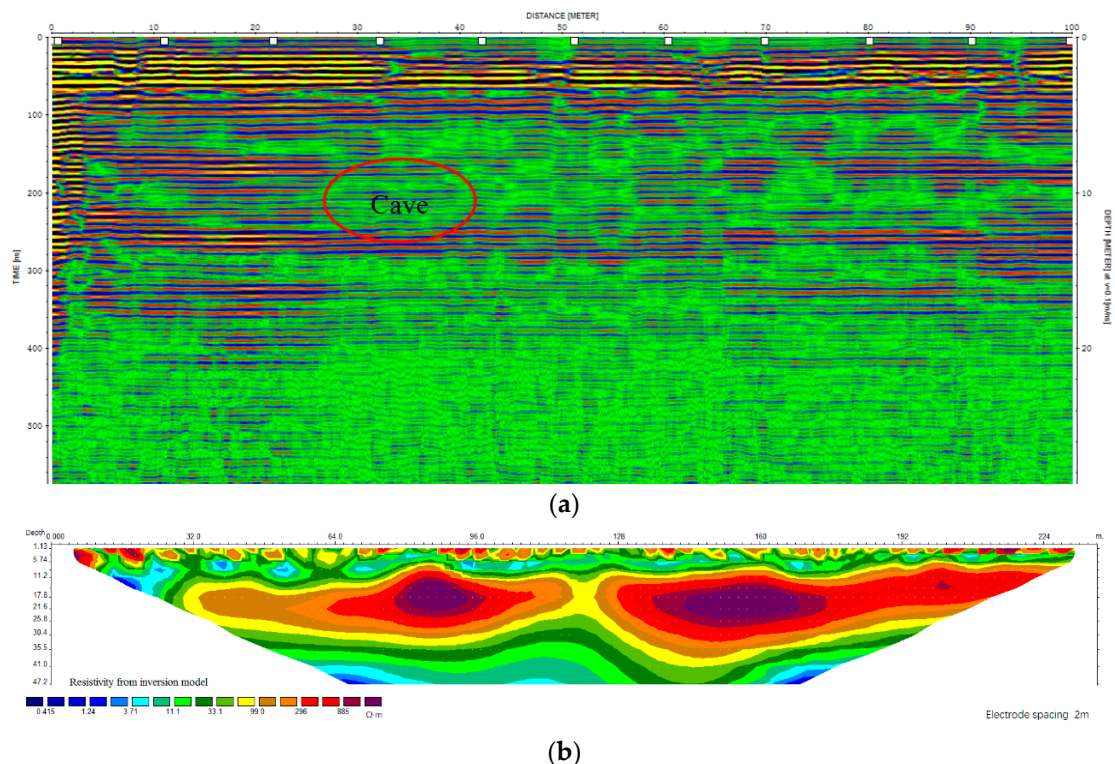
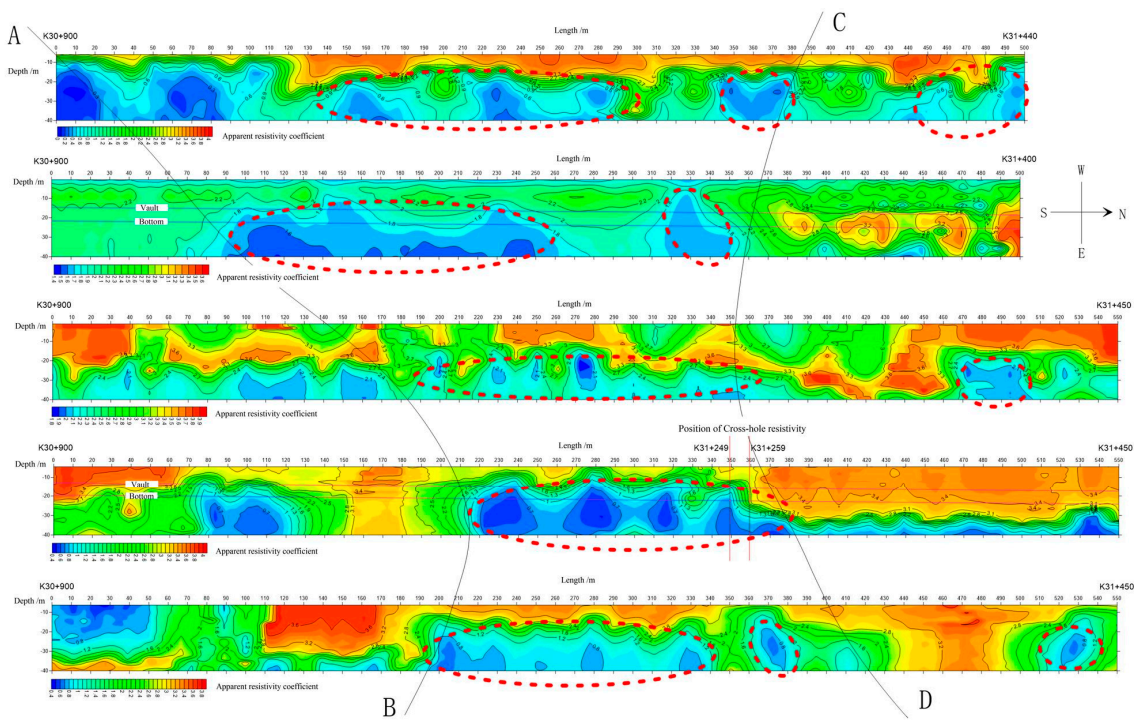
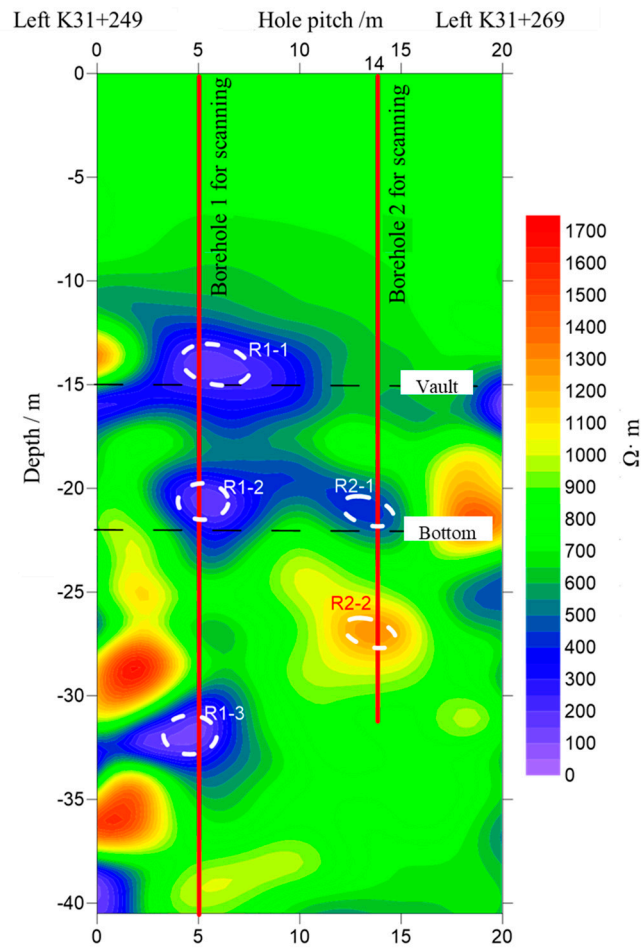


Figure 13. Cont.



(c)



(d)

Figure 13. Cont.

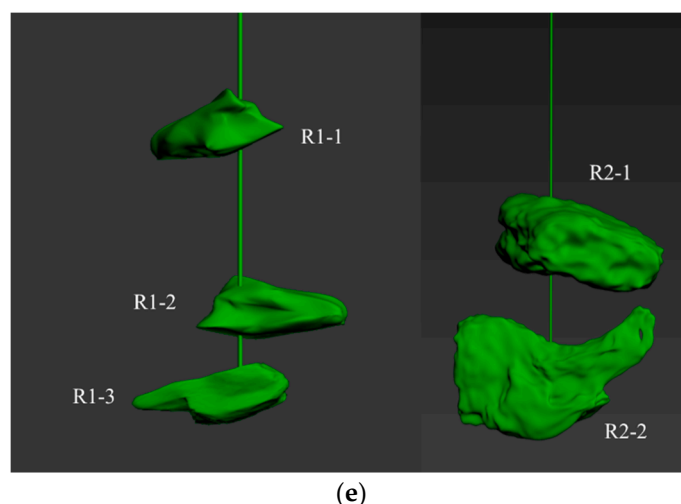


**Figure 13.** Results (a) GPR method; (b) Cross-section of high-density electrical method; (c) Comprehensive interpretation of transient electromagnetic method; (d) Cross-section of cross-hole resistivity CT method; (e) Scanning results.

### 5.2. Depth of Karst Caves

The depth of karst caves along Jinan metro lines are shown in Table 3, and the corresponding curve was drawn, as shown in Figure 14. As can be seen from the figure that most depths of karst caves of Jinan metro R1 line are in the range of  $-25$ – $0$  m, accounting for 91.46%, and that depths below  $-25$  m account for 8.54%, indicating that development mainly took place in shallow karst. To be specific, karst development concentrates on depths between  $-20$  m– $-15$  m, accounting for 31.78%, followed by the range of  $-15$  m– $-10$  m, which accounts for 23.26%. The proportions of karst caves with depth between  $-10$  m and  $-5$  m, and  $-25$  m and  $-20$  m are basically the same, while the percentage of caves developed in the Quaternary strata and deep limestone areas is extremely small. The development regularity of karst caves along R2 line shows the same trend with that of R1 line. This is mainly because the erosion effect of groundwater activity is intense in shallow karst areas. The depths of shield tunnel are basically between  $-20$  m and  $-10$  m, falling into the range with concentrated karst development. Therefore, under the long-term groundwater action, the scale of karst cave may be further expanded, affecting the stability of shield tunnel.

**Table 3.** Number of karst caves in various depths.

Depth Range (–m)	Number of Karst Caves	Proportion (%)
0–5	2	1.06
5–10	25	13.23
10–15	34	17.99
15–20	47	24.87
20–25	28	14.81
25–30	11	5.82
30–35	7	3.7
35–40	6	3.17
In Total	189	100.00

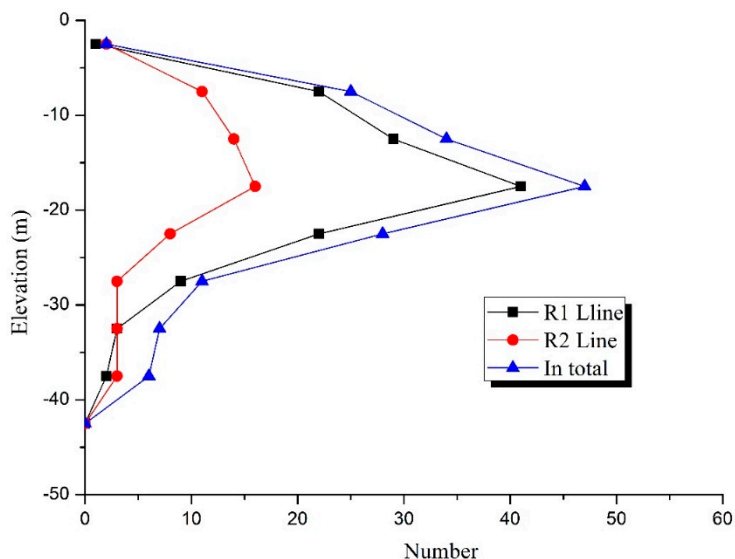


Figure 14. Number of karst caves in various depths.

5.3. Spatial Relationship between Caves and Shield Tunnels

According to situation of karst caves exposed along the Jinan Metro, the analysis of the positional relationship between the tunnel and the caves was carried out and the data in detail can be seen in Table 4 and Figure 15. The distribution is listed as follows:

- (1) There are 29 exposed karst caves above the tunnel roof, accounting for 22.48% of the total number. Among them, 20 karst caves are within the range of 0.5 time of the cave diameter above the tunnel roof; 7 karst caves are within 0.5 to 1 time of the cave diameter; 2 karst caves are within 1 to 2 times of the cave diameter. There are 21 exposed karst caves less than 1 m above the tunnel roof, 8 caves larger than 1 m, 3 caves larger than 2 m, and 2 caves larger than 3 m.
- (2) There are 65 exposed karst caves within the range of tunnel, accounting for 50.39% of the total number. Among them, 34 exposed karst caves are less than 1 m, 31 caves larger than 1 m, 19 caves larger than 2 m, and 15 caves larger than 3 m.
- (3) There are 35 exposed karst caves below the tunnel floor, accounting for 27.13% of the total number. Among them, 18 karst caves are within the range of 0.5 time of the cave diameter below the tunnel floor; 11 karst caves are within 0.5 to 1 time of the cave diameter; 4 karst caves are within 1 to 2 times of the cave diameter; 2 karst caves are within 2 or more times of the cave diameter below the tunnel floor. There are 24 exposed karst caves less than 1 m below the tunnel floor, 11 caves larger than 1 m, 7 caves larger than 2 m, and 6 caves larger than 3 m.

Table 4. Statistics of relative position of karst caves and shield tunnels.

Relation between Caves and Tunnels	Distance between Caves and Tunnels		Size of Caves	
	Time of Cave Diameter	Number	Height (m)	Number
Caves above tunnel	≤0.5 D	20	≤1	21
	0.5–1 D	7	1–2	5
	1–2 D	2	2–3	1
	>2 D	0	>3	2
Caves in tunnel	-	-	≤1	34
	-	-	1–2	12
	-	-	2–3	4
	-	-	>3	15
Caves below tunnel	≤0.5 D	18	≤1	24
	0.5–1 D	11	1–2	4
	1–2 D	4	2–3	1
	>2 D	2	>3	6

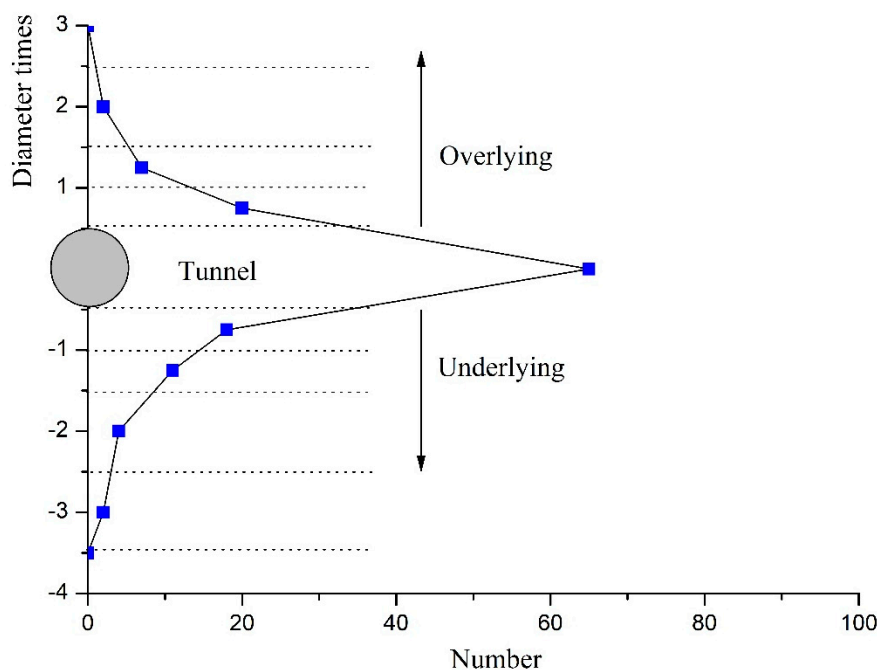


Figure 15. Relative position of karst caves and shield tunnels.

## 6. Conclusions and Discussion

Based on the systematic analysis of the hydrogeological characteristics of Jinan area, this paper studies the karst development conditions and mechanisms in areas where Jinan Metro runs through. We try to propose a comprehensive exploration system for karst area and reveal the karst development scale, filling types, and spatial distribution features along the Jinan Metro lines.

The topography and geomorphology, lithology distribution, hydrogeology, and tectonic influence of Jinan are systematically analyzed. With reference to the geological characteristics of Jinan and the karst development conditions, the karst development conditions and feedback mechanism along Jinan Metro lines were analyzed. Furthermore, formation and developmental mechanism of direct karst, indirect karst and confined karst were proposed. Accordingly, when Jinan Metro run through the indirect karst area, it needs to be noted that karst collapse can cause great damage to surface buildings, roads, and pedestrians. In the area of pressure-bearing karst distribution, due to a certain water pressure in the cave, special attention should be paid to protecting the thickness of the rock wall during the shield tunneling. The geological analysis can provide a geological basis to the planning and design of metro line and the safety of shield tunnel in Jinan.

The karst development scale and filling type characteristics along Jinan Metro are analyzed. The results show that the karst caves are mainly small- and medium-sized. It needs to be noted that there are several large-scale and water-filled caves along the subway. Due to confined water and weakening effect on rocks, it can easily cause water inrush hazard during shield tunneling.

According to karst development characteristics in areas where Jinan Metro runs through, a “shallow-deep” and “region-target” comprehensive exploration system of karst caves was proposed. The system solves the problem that a single method cannot meet the detection precision needs especially in complex geological conditions. The system makes full use of the advantages of multiple methods. Therefore, the potential karst caves in the shallow and regional along the Jinan subway line can be effectively explored. Furthermore, for the key areas, the refined exploration method has been adopted to achieve the quantitative acquisition and visual characterization of karst cave. The results demonstrate that laser scanning is an effective “target” method to reconstruct the shape of irregular karst caves based on the “area” exploration, which can determine the accurate parameters including position, depth and volume, and so on. These parameters can be beneficial for the efficient and high-quality treatment of karst caves. Compared to single method, the system proposed in this

paper can improve the detection efficiency and accuracy, which will provide guidance for similar metro projects.

Based on the comprehensive exploration system, the spatial positional relation between karst development elevation and the shield tunnel was statistically analyzed. The results show that karst caves in the range of tunnel structure account for about 50.39%, that karst caves above tunnel structure account for about 22.48%, and that karst caves below tunnel structure account for about 27.13%, respectively. When the karst cave is overlying above the tunnel, it is easy to cause karst collapse. When the cave is situated under the tunnel, excessive settlement of the karst foundation is likely to occur. Water inrush hazard can occur when the rock thickness between the tunnel face and the cave is too small. Therefore, based on the statistics of the positional relationship between the cave and the tunnel, we can take preventive measures to ensure the safety of the project in advance accordingly.

**Author Contributions:** Methodology, S.S. (Shangqu Sun); Writing-Original Draft Preparation, L.L.; Investigation, J.W.; Validation, S.S. (Shuguang Song); Data Curation, Z.F. and X.B.; Writing-Review & Editing, S.S. (Shaoshuai Shi) and H.J.

**Funding:** This research was funded by [National Science Fund for Excellent Young Scholars] grant number [51722904]; [National Natural Science Foundation Item] grant number [51679131] and [51479106]; [National Natural Science Foundation of China] grant number [51809158] and [51709160]; [Shandong Province Science Foundation for Distinguished Young Scholars] grant number [JQ201611]; [China Postdoctoral Science Foundation] grant number [2018M630780]; [Shandong Provincial Natural Science Foundation, China] grant number [ZR2017QEE009] and [ZR2018BEE045].

**Conflicts of Interest:** The authors declare no conflict of interest.

## References

1. Wu, H.N.; Huang, R.Q.; Sun, W.J.; Shen, S.L.; Xu, Y.S.; Liu, Y.B.; Du, S.J. Leaking behaviour of shield tunnels under the Huangpu river of Shanghai with induced hazards. *Nat. Hazards* **2014**, *70*, 1115–1132. [[CrossRef](#)]
2. Tan, Y.; Wang, D.L. Characteristics of a large-scale deep foundation pit excavated by central-island technique in Shanghai soft clay. I: Bottom-up construction of the central cylindrical shaft. *ASCE J. Geotech. Geoenviron. Eng.* **2013**, *139*, 1875–1893. [[CrossRef](#)]
3. Tan, Y.; Wang, D.L. Characteristics of a large-scale deep foundation pit excavated by central-island technique in Shanghai soft clay. II: Top-down construction of the peripheral rectangular pit. *ASCE J. Geotech. Geoenviron. Eng.* **2013**, *139*, 1894–1910. [[CrossRef](#)]
4. Shen, S.L.; Wu, H.N.; Cui, Y.J.; Yin, Z.Y. Long-term settlement behavior of the metro tunnel in Shanghai. *Tunn. Undergr. Space Technol.* **2014**, *40*, 309–323. [[CrossRef](#)]
5. Xu, Y.S.; Ma, L.; Shen, S.L.; Sun, W.J. Evaluation of land subsidence by considering underground structures that penetrate the aquifers of Shanghai, China. *Hydrogeol. J.* **2012**, *20*, 1623–1634. [[CrossRef](#)]
6. Xu, Y.S.; Ma, L.; Du, Y.J.; Shen, S.L. Analysis on urbanization induced land subsidence in Shanghai. *Nat. Hazards* **2012**, *63*, 1255–1267. [[CrossRef](#)]
7. Liao, S.M.; Liu, J.H.; Wang, R.L.; Li, Z.M. Shield tunneling and environment protection in Shanghai soft ground. *Tunn. Undergr. Space Technol.* **2009**, *24*, 454–465. [[CrossRef](#)]
8. Wang, W.; Gao, S.; Liu, L.; Wen, W.; Li, P.; Chen, J. Analysis on the safe distance between shield tunnel through sand stratum and underlying karst cave. *Geosyst. Eng.* **2018**. [[CrossRef](#)]
9. Zhang, Q.; Tian, S.; Mo, Y.; Dong, X.; Hao, S. An expert system for prediction of karst disaster in excavation of tunnels or underground structures through a carbonate rock area. *Tunn. Undergr. Space Technol.* **1993**, *8*, 373–378.
10. Yang, Y.S.; Wu, H.; Xu, J.F.; Yang, X.Q. Construction of shield tunnel in karst strata. *J. Railw. Eng. Soc.* **2007**, *7*, 56–60. (In Chinese)
11. Ju, S.J.; Zhu, W.B. Study on geological investigation methods for shield tunneling in mixed ground. *Tunn. Constr.* **2007**, *27*, 10–14. (In Chinese)
12. Li, S.C.; Zhou, Z.Q.; Li, L.P.; Xu, Z.H.; Zhang, Q.Q.; Shi, S.S. Risk assessment of water inrush in karst tunnels based on attribute synthetic evaluation system. *Tunn. Undergr. Space Technol.* **2013**, *38*, 50–58. [[CrossRef](#)]

13. Li, X.; Li, Y. Research on risk assessment system for water inrush in the karst tunnel construction based on GIS: Case study on the diversion tunnel groups of the Jinping II hydropower station. *Tunn. Undergr. Space Technol.* **2014**, *40*, 182–191. [[CrossRef](#)]
14. Shen, S.L.; Xu, Y.S. Numerical evaluation of land subsidence induced by groundwater pumping in Shanghai. *Can. Geotech. J.* **2011**, *48*, 1378–1392. [[CrossRef](#)]
15. Shen, S.L.; Wang, Z.F.; Sun, W.J.; Wang, L.B.; Horpibulsuk, S. A field trial of horizontal jet grouting using the composite-pipe method in the soft deposits of Shanghai. *Tunn. Undergr. Space Technol.* **2013**, *35*, 142–151. [[CrossRef](#)]
16. Cui, Q.L.; Wu, H.N.; Shen, S.L.; Xu, Y.S.; Ye, G.L. Chinese karst geology and measures to prevent geohazards during shield tunnelling in karst regions with caves. *Nat. Hazards* **2015**, *77*, 129–152. [[CrossRef](#)]
17. Font-Capo, J.; Pujades, E.; Vázquez-Suñé, E.; Carrera, J.; Velasco, V.; Montfort, D. Assessment of the barrier effect caused by underground constructions on porous aquifers with low hydraulic gradient: A case study of the metro construction in Barcelona, Spain. *Eng. Geol.* **2015**, *196*, 238–250. [[CrossRef](#)]
18. Pujades, E.; López, A.; Carrera, J.; Vázquez-Suñé, E.; Jurado, A. Barrier effect of underground structures on aquifers. *Eng. Geol.* **2012**, *145–146*, 41–49. [[CrossRef](#)]
19. Wang, G.F.; Wu, Y.X.; Lu, L.H.; Li, G.; Shen, J.S. Investigation of the geological and hydrogeological environment with relation to metro system construction in Jinan, China. *Bull. Eng. Geol. Environ.* **2017**, 1–20. [[CrossRef](#)]
20. Shen, S.L.; Wu, Y.X.; Xu, Y.S.; Hino, T.; Wu, H.N. Evaluation of hydraulic parameter based on groundwater pumping test of multiaquifer system of Tianjin. *Comput. Geotech.* **2015**, *68*, 196–207. [[CrossRef](#)]
21. Wu, Y.X.; Shen, S.L.; Wu, H.N.; Xu, Y.S.; Yin, Z.Y.; Sun, W.J. Environmental protection using dewatering technology in a deep confined aquifer beneath a shallow aquifer. *Eng. Geol.* **2015**, *196*, 59–70. [[CrossRef](#)]
22. Williams, P.W. The role of the subcutaneous zone in karst hydrology. *J. Hydrol.* **1983**, *61*, 45–67. [[CrossRef](#)]
23. Clemens, T.; Hückinghaus, D.; Liedl, R.; Sauter, M. Simulation of the development of karst aquifers: Role of the epikarst. *Int. J. Earth Sci.* **1999**, *88*, 157–162. [[CrossRef](#)]
24. Williams, P.W. The role of the epikarst in karst and cave hydrogeology: A review. *Int. J. Speleol.* **2008**, *37*, 1–10. [[CrossRef](#)]
25. Huang, X.; Li, S.; Xu, Z.; Guo, M.; Chen, Y. Assessment of a Concealed Karst Cave's Influence on Karst Tunnel Stability: A Case Study of the Huaguoshan Tunnel, China. *Sustainability* **2018**, *10*, 2132. [[CrossRef](#)]



© 2018 by the authors. Licensee MDPI, Basel, Switzerland. This article is an open access article distributed under the terms and conditions of the Creative Commons Attribution (CC BY) license (<http://creativecommons.org/licenses/by/4.0/>).